Investigating Potential Causes for the Prediction of Spurious Magnetopause Crossings at Geosynchronous Orbit in MHD Simulations

Pauline M. Dredger[1], Ramon E. Lopez[1], Yaireska M. Collado-Vega[2], Shreeya Khurana[3], Lutz M. Rastaetter[2]

[1]University of Texas at Arlington, Arlington, TX
[2]NASA Goddard Space Flight Center, Greenbelt, MD, Space Weather Laboratory, Code 674, Greenbelt, MD
[3]Carnegie Mellon University, Pittsburgh, PA

Key Points:

- MHD models driven by OMNI solar wind can wrongly predict magnetopause motion if solar wind observed at L1 does not reach the magnetosphere.
- The models predict magnetopause motion better if the driver of the motion is solar wind density than when the driver is a negative IMF Bz.
- Coupling the MHD codes to a ring current model for storm-time events results in significantly better predictions of magnetopause location.

Corresponding author: Pauline M. Dredger, pauline.dredger@mavs.uta.edu

Abstract

During intense geomagnetic storms, the magnetopause can move in as far as geosynchronous orbit, leaving the satellites in that orbit out in the magnetosheath. Spacecraft operators turn to numerical models to predict the response of the magnetopause to solar wind conditions, but the predictions of the models are not always accurate. This study investigates four storms with a magnetopause crossing by at least one GOES satellite, using four magnetohydrodynamic models at NASA's Community Coordinated Modeling Center (CCMC) to simulate the events, and analyzes the results to investigate the reasons for errors in the predictions. Two main reasons can explain most of the erroneous predictions. Firstly, the solar wind input to the simulations often contains features measured near the L1 point that did not eventually arrive at Earth; incorrect predictions during such periods are not the fault of the models. Secondly, while the models do well when the primary driver of magnetopause motion is a variation in the solar wind density, they tend to overpredict or underpredict the Birkeland currents during times of strong negative IMF B_z, leading to poorer prediction capability. Coupling the MHD codes to a ring current model, when such a coupling is available, generally will improve the predictions but will not always entirely correct them. More work is needed to fully characterize the response of each code under strong southward IMF conditions as it relates to prediction of magnetopause location.

Plain Language Summary

The magnetopause is the boundary that separates the region dominated by Earth's magnetic field from the solar wind. Plasma and magnetic field conditions are very different on either side of the magnetopause, which can cause problems for satellites when the boundary moves and they find themselves in a different region of space than expected. Numerical models of the magnetosphere are used to predict the motion of the magnetopause, which moves based on the driving of the solar wind, but such predictions do not always correspond to real-life observations. This study compares predictions from four different models to observations from spacecraft that crossed the magnetopause during a handful of events with intense solar wind conditions, to determine the reasons that simulation results could be incorrect. The first source of error is the uncertainty in solar wind input to the models. The second source of error is a difference in the response of the codes to different solar wind parameters. Coupling the magnetosphere models to models that add the physics of specific magnetosphere regions can help to improve the accuracy of the overall predictions of magnetopause motion.

1 Introduction

The magnetopause, the boundary between the magnetosphere and the shocked solar wind in the magnetosheath, separates two regions of very different plasma and magnetic field conditions. In general, the magnetosheath is turbulent, with dense plasma and magnetic field that vary with the arrival of the solar wind, while inside the magnetosphere Earth's magnetic field dominates and plasma densities are much lower. The balance of plasma pressure from the magnetosheath and magnetic pressure from the terrestrial magnetic field determines, in the most basic approximation, the instantaneous location of the magnetopause, which varies with the two pressures (Martyn, 1951). High solar wind dynamic pressure in the magnetosheath will force the boundary inward towards Earth from the outside. On the other hand, a strong southward interplanetary magnetic field (IMF) components will increase the Region 1 field-aligned currents and the nightside cross-tail current, creating fringe fields opposite to Earth's magnetic field and thus weakening it, which reduces the outward magnetic pressure from the inside and allows the magnetopause to move closer to Earth (Maltsev & Lyatsky, 1975; Maltsev et al., 1996; Sibeck

et al., 1991; Wiltberger et al., 2003). A numerical model of the magnetosphere must reproduce these phenomena if it is to accurately predict magnetopause position.

The ring current, which is strongest during a geomagnetic storm, can also affect the position of the magnetopause. As ions are injected from the tail into the inner magnetosphere, they join the ring current and flow clockwise around Earth (as seen from the north); because of the direction of flow, more particles are lost to the dawn sector magnetopause than to the dusk sector, and the ring current becomes asymmetrical. The resulting partial ring current closes along magnetic field lines as the Region 2 field-aligned current, flowing into the polar cap on the dusk side and out on the dawn side. The stronger thermal pressure from the ions in the partial ring current in the dusk sector causes the magnetopause to be farther away from Earth than it is in the dawn sector (Dmitriev et al., 2011).

During times of quiet solar wind, the magnetopause is several Earth radii away from geosynchronous orbit, where many commercial and scientific satellites are located, and so these spacecraft remain inside the magnetosphere; when, on the other hand, a geomagnetic storm arrives at Earth, the location of the boundary is much more variable (Bonde et al., 2018). Operators of satellites orbiting near Earth rely on predictions of magnetopause location to let them know if their spacecraft might cross the boundary, particularly if the spacecraft use magnetic torquing for attitude adjustments (Sibeck, 1995). Often to make these predictions, satellite operators use the magnetohydrodynamic (MHD) models available at the CCMC: the Lyon-Fedder-Mobarry simulation (LFM), the Space Weather Modeling Framework (SWMF), the Open Geospace General Circulation Model (OpenGGCM), and the Grand Unified Magnetosphere-Ionosphere Circulation Model (GUMICS). While empirical models of magnetopause position exist, physics-based models can provide a better (if imperfect) prediction capability during extreme magnetic storms (Lopez et al., 2007). Collado-Vega et al. (2022) conducted a study examining the performance of these four models in predicting magnetopause location for eight storms; specifically, the study looked for correctly simulated magnetopause encounters at the locations of GOES 13 and 15, both at geosynchronous orbit. They found that SWMF and GUMICS tended to underpredict magnetopause motion in response to strong solar wind conditions, while LFM and OpenGGCM predicted both correct and spurious magnetopause crossings. In order to better understand the models' predictive capabilities, including under what conditions their use is appropriate, this study investigates possible causes for their incorrect predictions, in particular the overpredictions of LFM and OpenGGCM, by considering the four events in the Collado-Vega paper in which GOES actually crossed the magnetopause.

2 Methodology

This study primarily uses the geocentric solar ecliptic (GSE) coordinate system. In GSE coordinates, X points along the Earth-sun line and Z is perpendicular to the ecliptic plane, where positive Z points northward. Y completes the right-handed coordinate system, with positive Y in the duskward direction.

To determine the time at which a satellite crosses the magnetopause, the following method was used. Earth's magnetic field points northward, so a magnetometer will always read a positive B_z while inside the magnetopause. If the incoming IMF has a negative Z-component, the compressed B_z in the sheath will be negative. Consequently, in magnetometer data, B_z will rotate from positive (negative) to negative (positive) as the spacecraft crosses the boundary into the magnetosheath (magnetosphere). The spacecraft encounters the magnetopause at the moment the magnetometer reads $B_z = 0$ nT. All the events in this study had strong southward IMF components, so magnetopause crossings in the relevant data were identified in this way.

For this study, four events were chosen in which solar wind conditions pushed the magnetopause so far towards Earth that it reached geosynchronous orbit and crossed over one or both of GOES 13 and 15. GOES 13 and 15 are part of NOAA's Geostationary Operational Environmental Satellite program and fly in geosynchronous orbits. During the events of this study, GOES 13 was located at 75 degrees West and GOES 15 was located at 135 degrees West, which means that GOES 13 was always four hours ahead of GOES 15 in local time.

Each event was simulated using all four magnetospheric models at the CCMC, without a ring current and using auroral conductances in order to compare the models as fairly as possible, since the couplings available vary among the codes. After these initial runs, the simulations for certain events were repeated with the MHD codes coupled to a ring current model where such a coupling was available at the CCMC. The four models used in this study are the LFM model, the SWMF, OpenGGCM, and GUMICS. These are briefly described here with their various possible couplings, as available at the CCMC.

LFM solves the semi-conservative MHD equations on a stretched spherical grid and uses its Magnetosphere-Ionosphere Coupler/Solver (MIX) to calculate the ionospheric electrostatic potential (Lyon et al., 2004; Merkin & Lyon, 2010). LFM can also couple with the Rice Convection Model (RCM), a bounce average drift kinetic model of the inner magnetosphere that adds ring current physics (Wolf et al., 1982; Toffoletto et al., 2003). The version of LFM-MIX coupled to RCM is available for use at the CCMC.

SWMF includes a number of modules that simulate various parts of the space weather system (Tóth et al., 2005; Tóth et al., 2012). The magnetosphere part of the framework (SWMF Global Magnetosphere module) uses the Block-Adaptive-Tree-Solarwind-Roe-Upwind-Scheme (BATS-R-US), which solves the conservative MHD equations on an adaptive grid (Powell et al., 1999). The SWMF Ionosphere Electrodynamics (IE) module uses the field-aligned currents from BATS-R-US to calculate the ionospheric potentials and conductances. SWMF request runs on the CCMC couple BATS-R-US with the two-dimensional IE potential solver and can include RCM. Runs used in this study used the version of the code implemented on the website in 2014.

OpenGGCM solves the semi-conservative MHD equations on a stretched Cartesian grid and maps the field-aligned currents onto a sphere within the inner boundary to a convection potential solver. OpenGGCM can also be coupled to RCM, but this coupling was not used in this work (Raeder et al., 2001, 2008; Cramer et al., 2017).

GUMICS-4, the version of GUMICS used here, couples an MHD model of the magnetosphere to an ionosphere model. The magnetosphere part of the code solves the conservative MHD equations on a refined hierarchically adaptive octogrid with a locally varying time-step while the simulation of the ionosphere is based on solving the height-integrated current continuity equation on a spherical surface with a prescribed grid point density highest in the auroral oval (Janhunen et al., 2012). GUMICS does not include a ring current component.

3 Results

3.1 Solar Wind Discrepancies

A closer examination of the individual events reveals that the solar wind input to the models may have caused some of the incorrect predictions. Because of the inhomogeneous nature of the solar wind, the conditions observed by a monitor at the first Lagrange point may differ significantly from the solar wind that actually impacts the magnetosphere. Comparisons between the OMNI dataset, which is composed of L1 observations from ACE and Wind propagated to a nominal bow shock position, and data from other spacecraft that were temporarily in the solar wind during the various events, re-

veal significant discrepancies between the datasets that explain several of the false alarms in the model predictions.

The first event, 2011 August 5, contains an error in the solar wind input that caused one of the models to predict a spurious magnetopause crossing by both GOES 13 and GOES 15. We see in Figure 1 the actual GOES observations and the model predictions plotted together. B_z from the model is plotted in GSE coordinates and the real data are in the cylindrical coordinate system used by GOES – the quantity plotted here is H_p, which is generally equivalent to B_z. Around 19:40 UT, B_z as predicted by OpenGGCM dips below 0 nT, indicating a magnetopause crossing by the satellite under consideration. LFM predicts an approach to the magnetopause around the same time but not a crossing. The solar wind from the OMNI dataset shows a density pulse from about 20 cm^{-3} to 40 cm^{-3} that caused the simulated magnetopause to move inward over the locations of GOES 13 and 15. This density pulse, observed at L1, does not seem to have actually reached Earth. The Honolulu magnetometer (which was near local noon at this time) responded to the density increases at 19:00 and at 20:00 UT, but it did not record a corresponding reaction to the 19:40 density pulse seen in the OMNI data (Figure 2). THEMIS B and C were in the solar wind at the time as shown in Figure 3, although they were between 50 and 60 R_E away from the Earth-Sun line. They did not record the increase in the solar wind density that Wind saw further upstream. The magnetometer and THEMIS observations, combined with the lack of a real magnetopause crossing at geosynchronous orbit, strongly suggest that the density pulse in the OMNI data at 19:40 UT did not impact the magnetopause. Thus, the erroneous predictions of magnetopause crossings were not necessarily mistakes by OpenGGCM but more likely the consequence of incorrect solar wind input.

A second event, 2011 September 26, tells a similar story. OpenGGCM predicts a magnetopause crossing at the location of GOES 13 shortly after 14:00 UT in response to a southward turning of IMF B_z accompanied by high proton densities in the OMNI data (Figure 4). This time, THEMIS B and C were well-positioned (Figure 5) to provide solar wind observations 170 R_E closer to Earth than Wind, less than 20 R_E from the Earth-Sun line. At the time when B_z in the OMNI data reached around -10 nT, the IMF B_z observed by THEMIS B and C was positive, with an overall difference of about 20 nT between THEMIS and OMNI. Proton densities at THEMIS B and C were also much less than those in OMNI by roughly 15 cm^{-3}, which could have contributed to pushing the magnetopause further inward. Incorrect solar wind input seems once again to explain the spurious crossing after 14:00 UT, although it is clearly not the only issue with the simulation results, given the other false crossings later in the day.

In addition to predicting false alarms, the models can also miss real crossings because of problems with the solar wind input. GOES 15 crossed the magnetopause right after 23:00 UT on 2017 September 7, but none of the models reproduced that crossing (Figure 6). THEMIS A, D, and E were intermittently in the solar wind between 23:00 and 23:30 UT, all within 2 R_E of the nose of the bow shock (Figure 7), and observed a negative IMF B_z of -20 nT or stronger right after 23:00 UT, while the IMF B_z from OMNI was -10 nT or weaker. Thus, even the two models that predicted the crossings minutes later, i.e. LFM and OpenGGCM, did not capture the initial crossing, probably due at least in part to this discrepancy between the two sets of solar wind observations. Unfortunately, the THEMIS spacecraft were not in the solar wind for very long and cannot be used to confirm the OMNI data later in the event.

3.2 Solar Wind Driver of Magnetopause Motion: IMF B_z vs. Density

Classification of the types of solar wind driver for the magnetopause crossings in each event leads to a further explanation of the false alarms and misses in the simulation results. The models seem to make good predictions when a sudden density increase

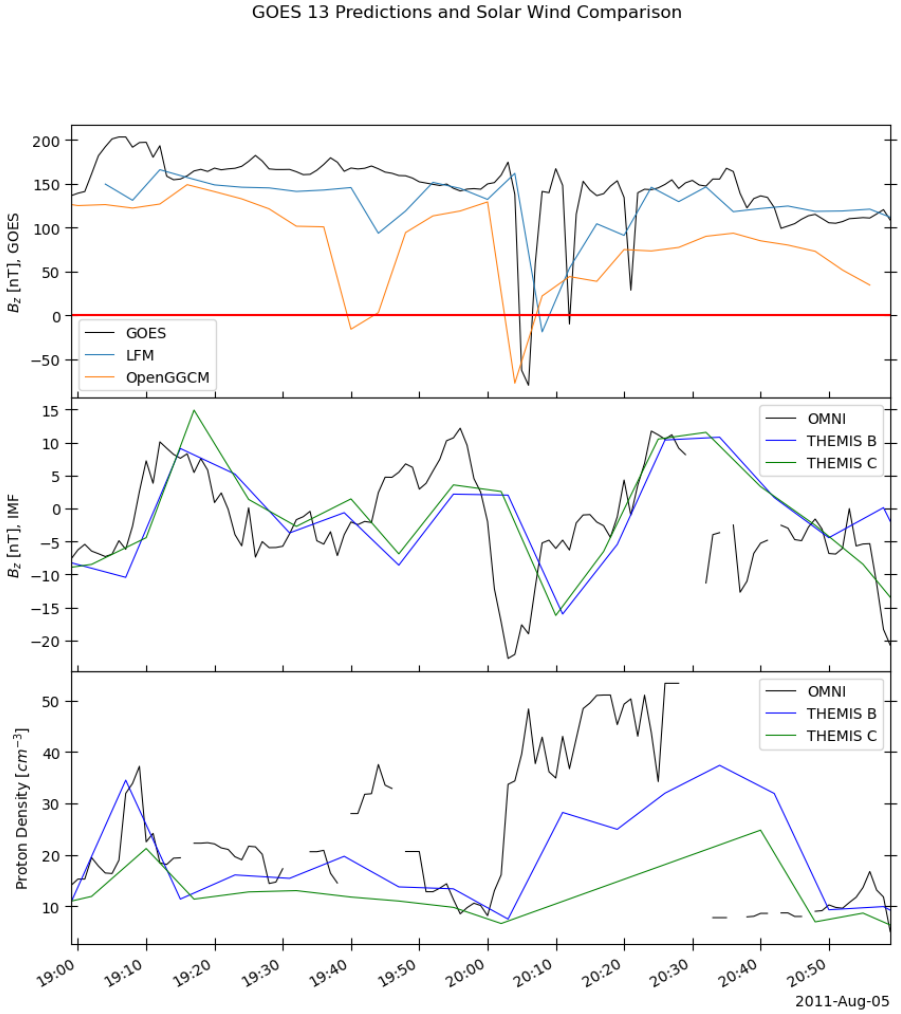

Figure 1. From top to bottom: (a) Observations of B_z from GOES 13 with predictions from LFM and OpenGGCM. (b) IMF B_z from OMNI compared with measurements from THEMIS B and C. Note that the propagation of OMNI data to a nominal bow shock does not necessarily correspond with the location of THEMIS B/C and so a shift in the time series is present. (c) Proton densities from OMNI and from THEMIS B/C.

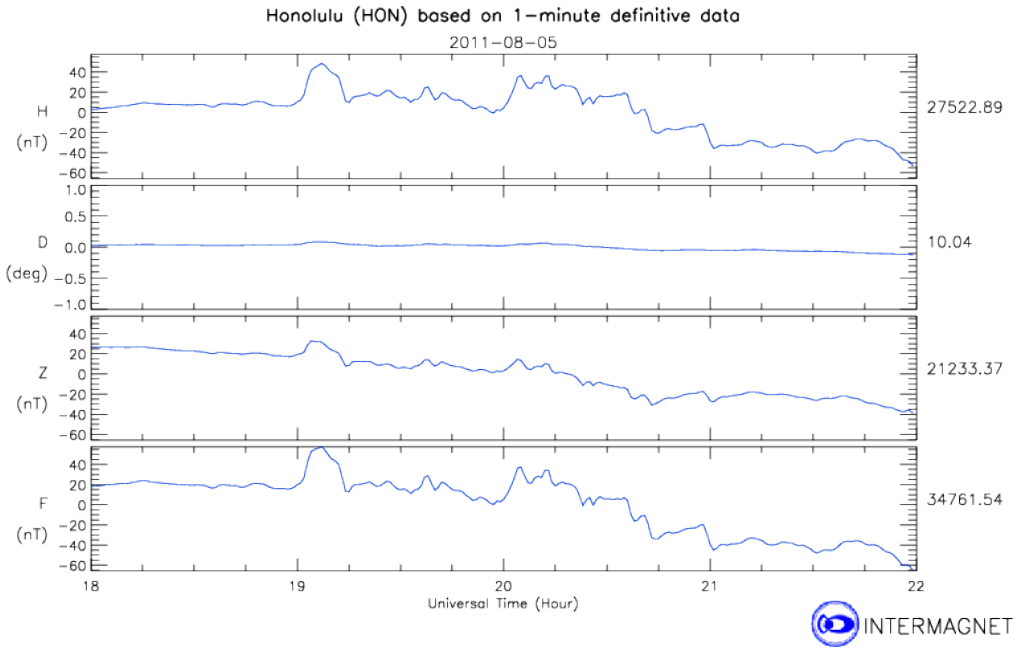

Figure 2. Magnetometer data from the Honolulu station. There is no real response to the 19:40 UT density pulse seen in OMNI, which may indicate that the pulse did not reach Earth (plot from Intermagnet).

drives the magnetopause inward, but perform poorly for events in which the magnetopause is eroded by the presence of a negative IMF B_z component. The predictions for 2011 September 26 follow this pattern. After the initial false crossing in OpenGGCM due to incorrect solar wind input right after 14:00 UT, both OpenGGCM and LFM predict a series of false alarms before and after the real crossing, which they do not reproduce. During the times of the spurious crossings, the solar wind proton densities are much lower than they were earlier in the event without much variation, but IMF B_z is strongly negative. Both models predict that the GOES satellites reentered the magnetosphere during the time of the real crossing, a brief encounter with the boundary that was probably caused by a relatively small density increase in the solar wind; the simulated magnetospheres seem to be responding more to the strong negative IMF B_z than to the bump in the densities.

The total field-aligned currents from each model on 2011 September 26 are plotted in Figure 8 alongside the currents from AMPERE. The two models that do not predict either real or spurious crossings, SWMF and GUMICS, have less current flowing into and out of the ionosphere than LFM or OpenGGCM, which have currents either similar to or greater than the AMPERE FACs. This event occurred near equinox, so the currents in both hemispheres are of similar strength. At the time of the real crossing, when AMPERE currents increase, the currents from LFM and SWMF actually decrease, probably in response to the northward turning of IMF B_z at this time, and GOES 13 in the LFM predictions exits the magnetosheath early. The modeled currents increase later around 18:00, when LFM and OpenGGCM predict more false crossings. During this period OMNI and THEMIS B and C all agree reasonably well, so it would seem that the solar wind input to the simulations is correct. The patterns of real and modeled currents correspond well to the real and modeled GOES observations, but the models re-

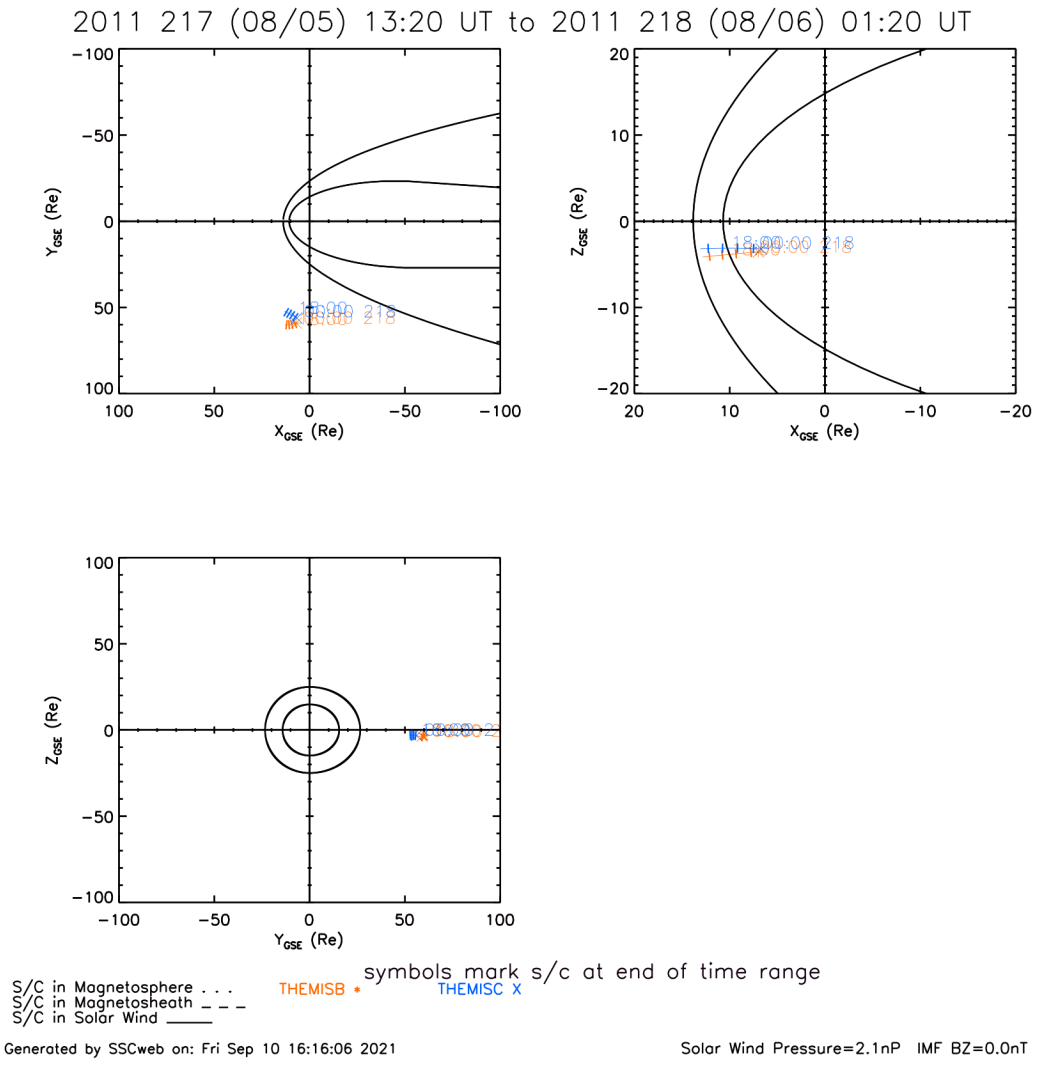

Figure 3. Locations of THEMIS B and C during the 2011 August 5 event. Although the two spacecraft are more than 50 R_E off the Earth-sun line, they are the only other source of solar wind observations for this event (plot from SSCWeb).

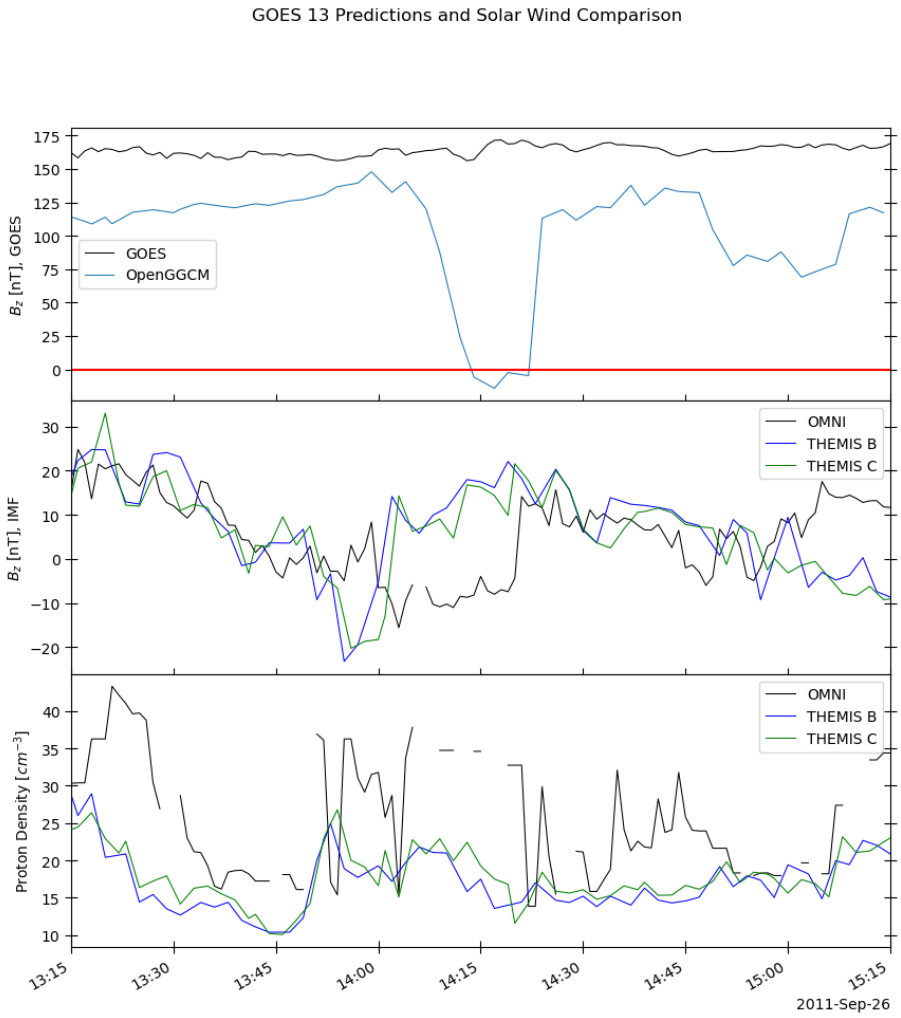

Figure 4. GOES 13 observations and corresponding OpenGGCM predictions, along with the solar wind from OMNI and THEMIS B/C for 2011 September 26. Even taking into account potential timing issues with the OMNI propagation, there are still significant differences in the OMNI and THEMIS sets of solar wind observations. The red horizontal line is included in this and any following GOES plots for ease of identifying magnetopause crossings, which occur at B_z = 0 nT under southward IMF conditions.

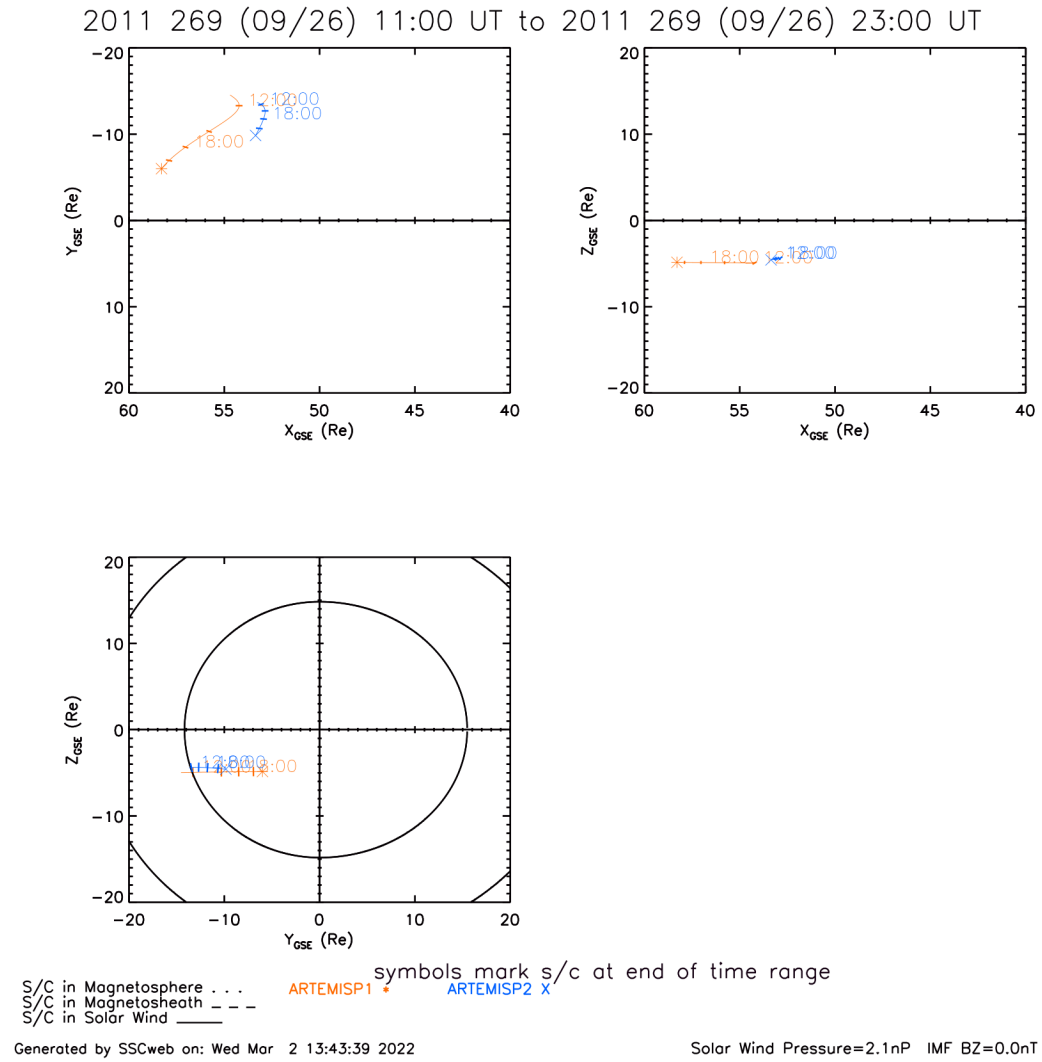

Figure 5. Locations of THEMIS B/C during the 2011 September 26 event. During this period, the two spacecraft were relatively close to the Earth-sun line and so their observations should be a good representation of the solar wind that impacted the bow shock (plot from SSCWeb).

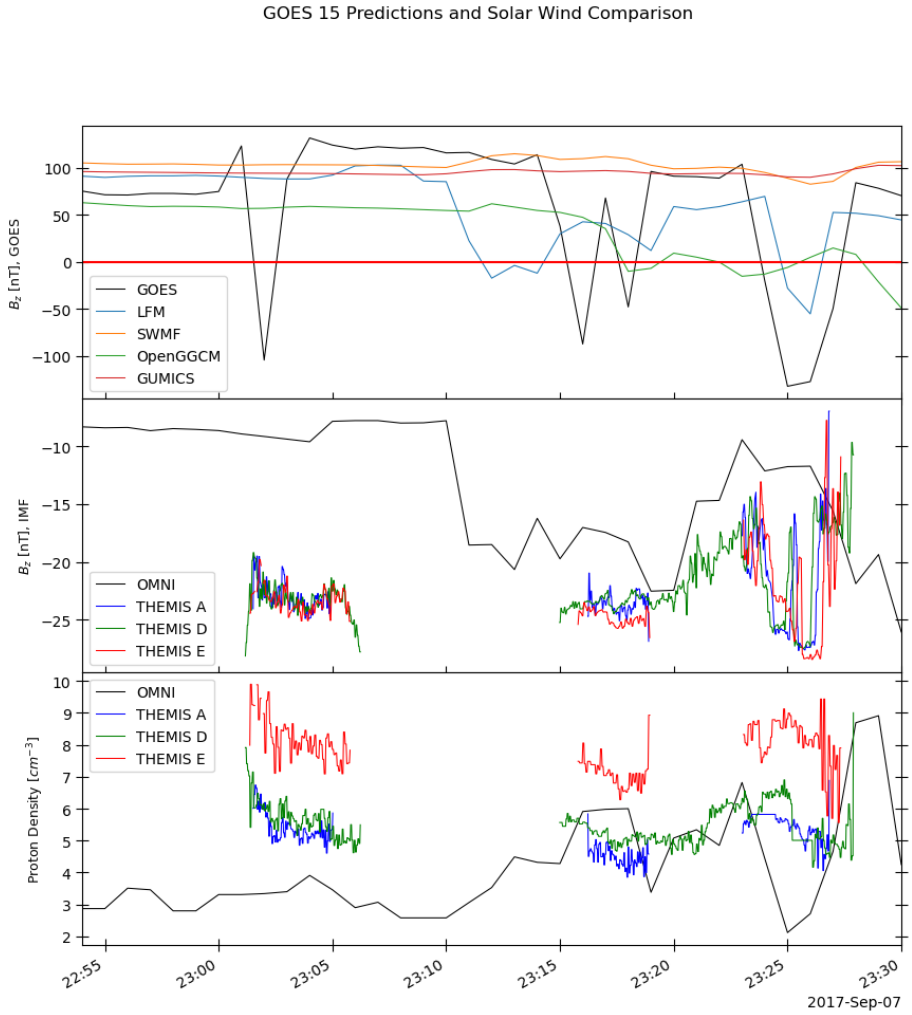

Figure 6. GOES 15 observations and model predictions with solar wind from OMNI and THEMIS A/D/E. THEMIS data are only plotted for the brief periods during which the spacecraft were in the solar wind. During this period the solar wind velocity (not shown here) changed drastically, so, as in previously discussed cases, there may be timing issues from the OMNI propagation.

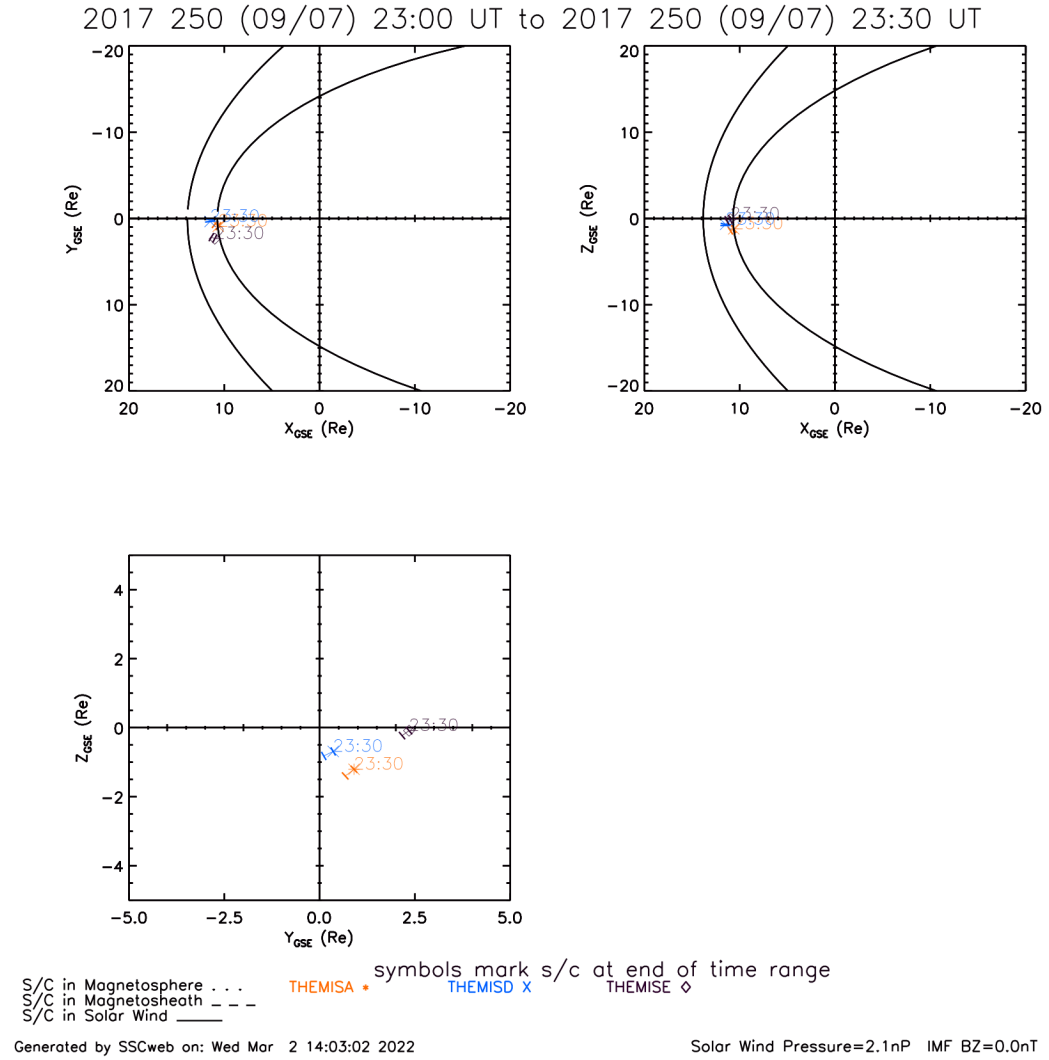

Figure 7. THEMIS A/D/E locations from 23:00 UT to 23:30 UT on 2017 September 7 (plot from SSCWeb).

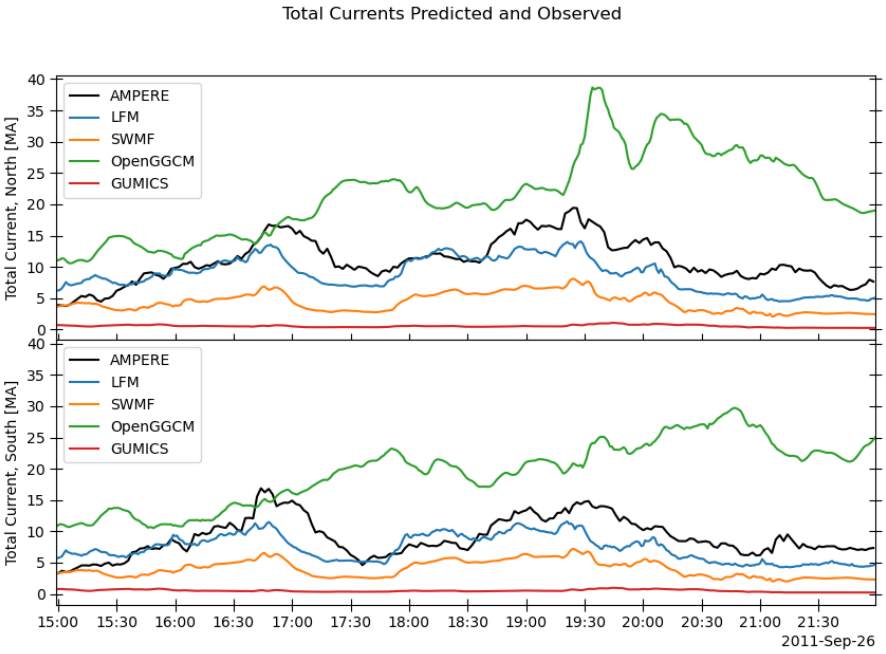

Figure 8. Total field-aligned currents in the northern and southern hemisphere from AMPERE and as predicted by the MHD models for 2011 September 26.

spond more to the IMF variations while the observations respond to changes in solar wind proton density.

The simulations of the geomagnetic storm of 2015 June 22 follow the same tendencies. All four models capture the magnetopause crossings by GOES 13 and 15 that lasted from right after 18:30 until about 20:00 UT; a sharp increase from 10 cm^{-3} to 60 cm^{-3} in proton density, accompanied by a southward turning of IMF B_z, which went from 0 nT to more than 15 nT, pushed the magnetopause all the way to geosynchronous orbit. Sustained high densities and increasingly stronger IMF B_z values that reached almost -40 nT kept GOES 13 and 15 in the magnetosheath until around 19:40 UT, when the northward turning of the IMF and a decrease in density to about 40 cm^{-3} allowed the magnetopause to move back outward again. This magnetopause motion is predicted reasonably well by the models, although the extent of the motion varies among the four simulations. LFM and OpenGGCM performed the best on this crossing, with SWMF close behind. However, around 21:00 UT, LFM and OpenGGCM predict a false crossing by GOES 13 (see Figure 9), in response to another change in IMF B_z, this time from 10 nT to -10 nT. There was a small jump in proton density at this time, but this variation was not significant compared to previous density increases and decreases. The Birkeland currents for the event are shown in Figure 10. At the time of the reversal of IMF B_z, the currents in both LFM and OpenGGCM increase, while the AMPERE currents are decreasing, especially in the summer hemisphere. The currents in the models are responding more strongly to IMF B_z than the real currents did in this event.

All the predicted crossings not due to incorrect solar wind input in the other two events, 2011 August 5 and 2017 September 7, can be explained in the same manner. Magnetopause motion driven primarily by increases of solar wind density tends to be predicted reasonably well, while strong southward IMF B_z values cause the models to over-

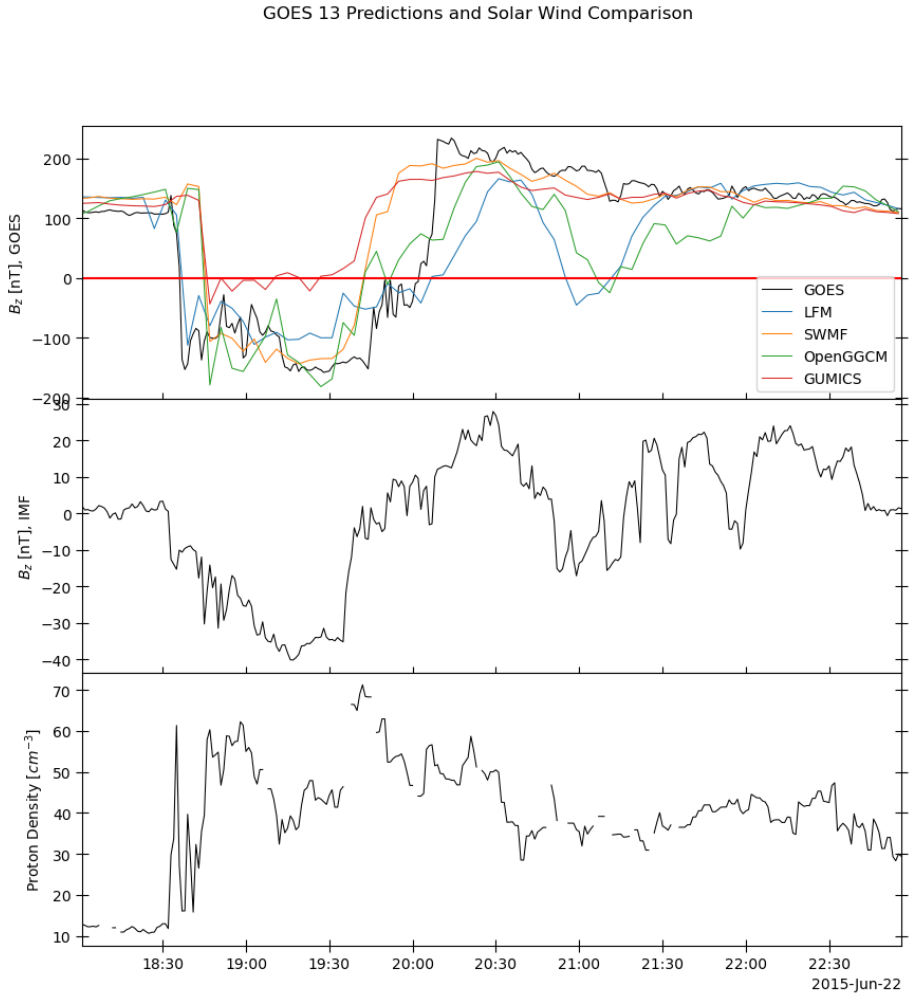

Figure 9. GOES 13 predictions and observations, with OMNI IMF B_z and proton densities.

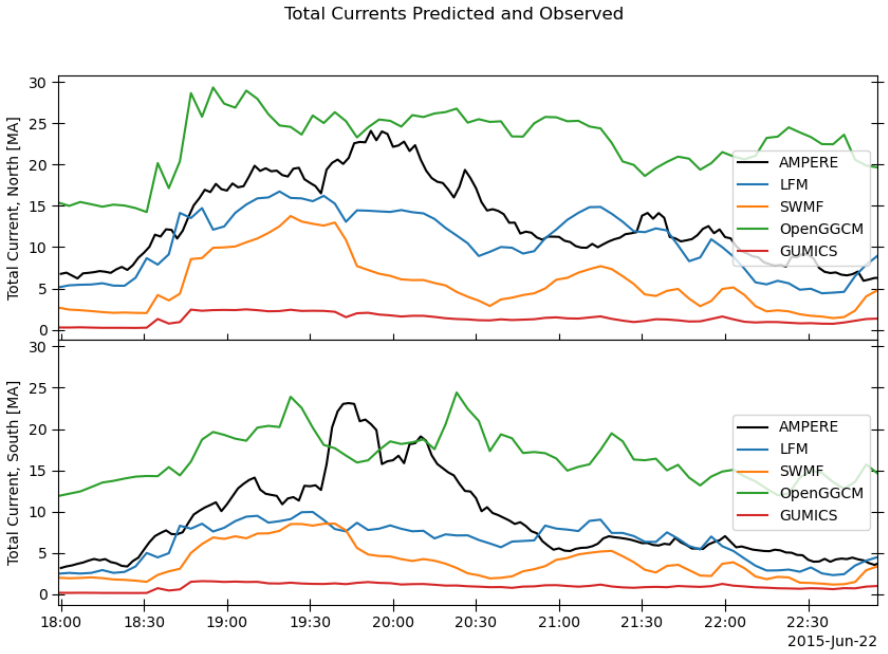

Figure 10. Total field-aligned currents in the northern and southern hemisphere from AMPERE and as predicted by the MHD models for 2015 June 22.

predict the inward motion of the boundary. Moreover, the simulated Birkeland currents during the false crossings do not match the currents seen in the AMPERE dataset.

3.3 Adding a Ring Current Model

Running LFM and SWMF coupled to the Rice Convection Model adds the effect of ring current physics, particularly during geomagnetic storms. For 2011 September 26, including the ring current greatly improves the LFM predictions and, to a lesser extent, those of SWMF, apart from the false alarms caused by incorrect solar wind densities in the first half of the event. The total current flowing into and out of the ionosphere is shown in Figure 11, which compares the AMPERE currents with those predicted by LFM and SWMF, both with and without the ring current. The simulation that included the ring current predicts the currents much better than the original run did. As a result, the predictions of magnetopause crossings at the GOES locations are more accurate. The ring current coupling helps SWMF as well, but the predicted currents are much weaker than the real currents and the model does not predict any magnetopause crossings.

The storm on 2011 August 5 responds similarly to the addition of the ring current. The LFM predictions improve at both the two GOES locations and for the Birkeland currents, although the simulation still underpredicts the periods of strongest current. SWMF with the ring current predicts one of the GOES 15 crossings, which before it had missed, and the predicted values for the Birkeland currents, while stronger, are still significantly lower than the AMPERE values (see Figure 12). The effect of including ring current physics is not as pronounced for this event as it is for the 2011 September event; this is, however, expected because the period of interest for the August event is early in the storm, before a strong ring current had time to form. The crossings during the 2017 September 7 storm also take place before SYM-H becomes strongly negative, so RCM has little effect on the predictions at the location of GOES 15. The later spurious crossing in

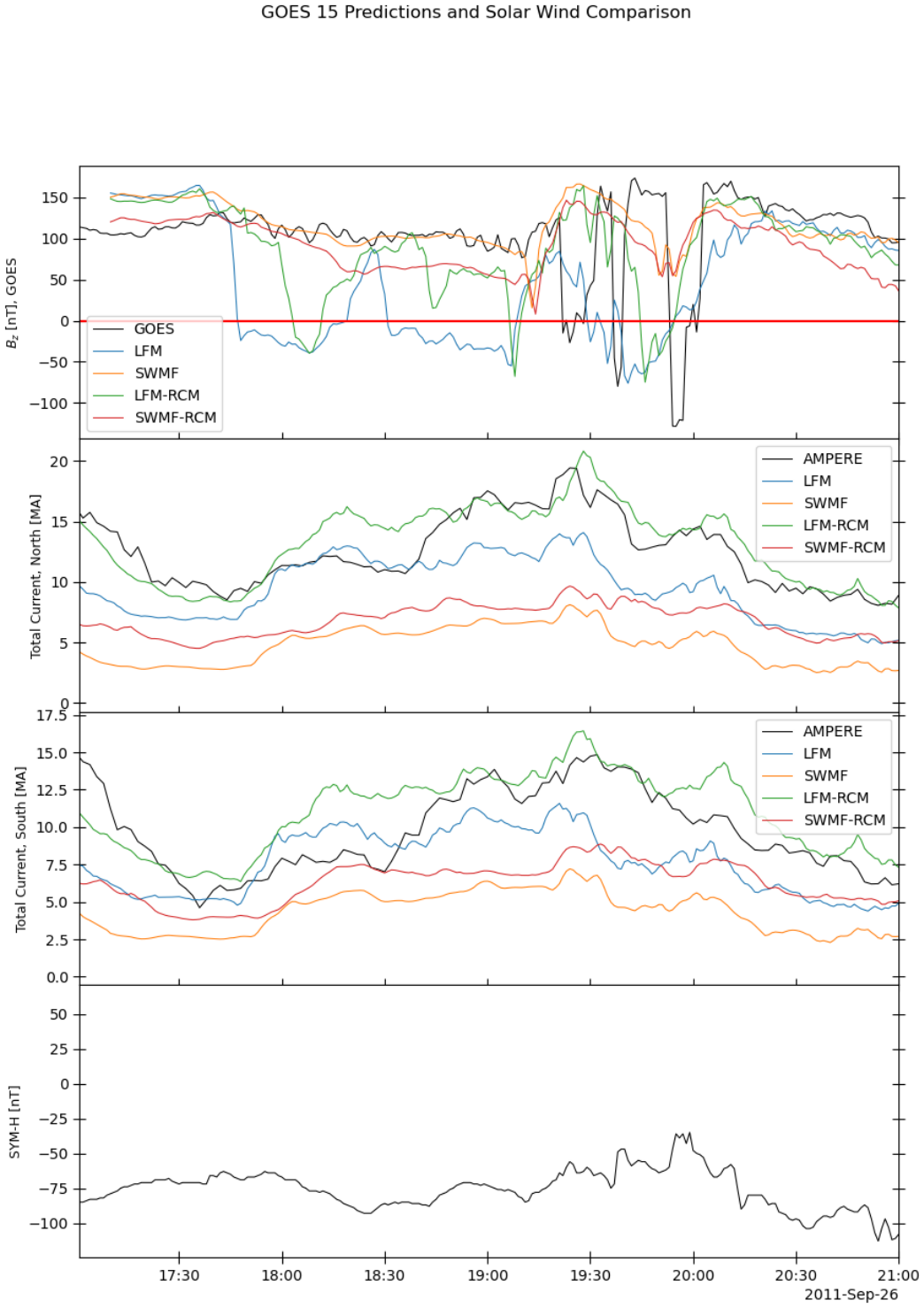

Figure 11. From top to bottom: (a) GOES 15 observations and the corresponding predictions from LFM and SWMF, with and without RCM; (b) total current into the northern hemisphere from AMPERE and the models; (c) total current into the southern hemisphere from AMPERE and the models; (d) SYM-H during the 2011 September 26 event.

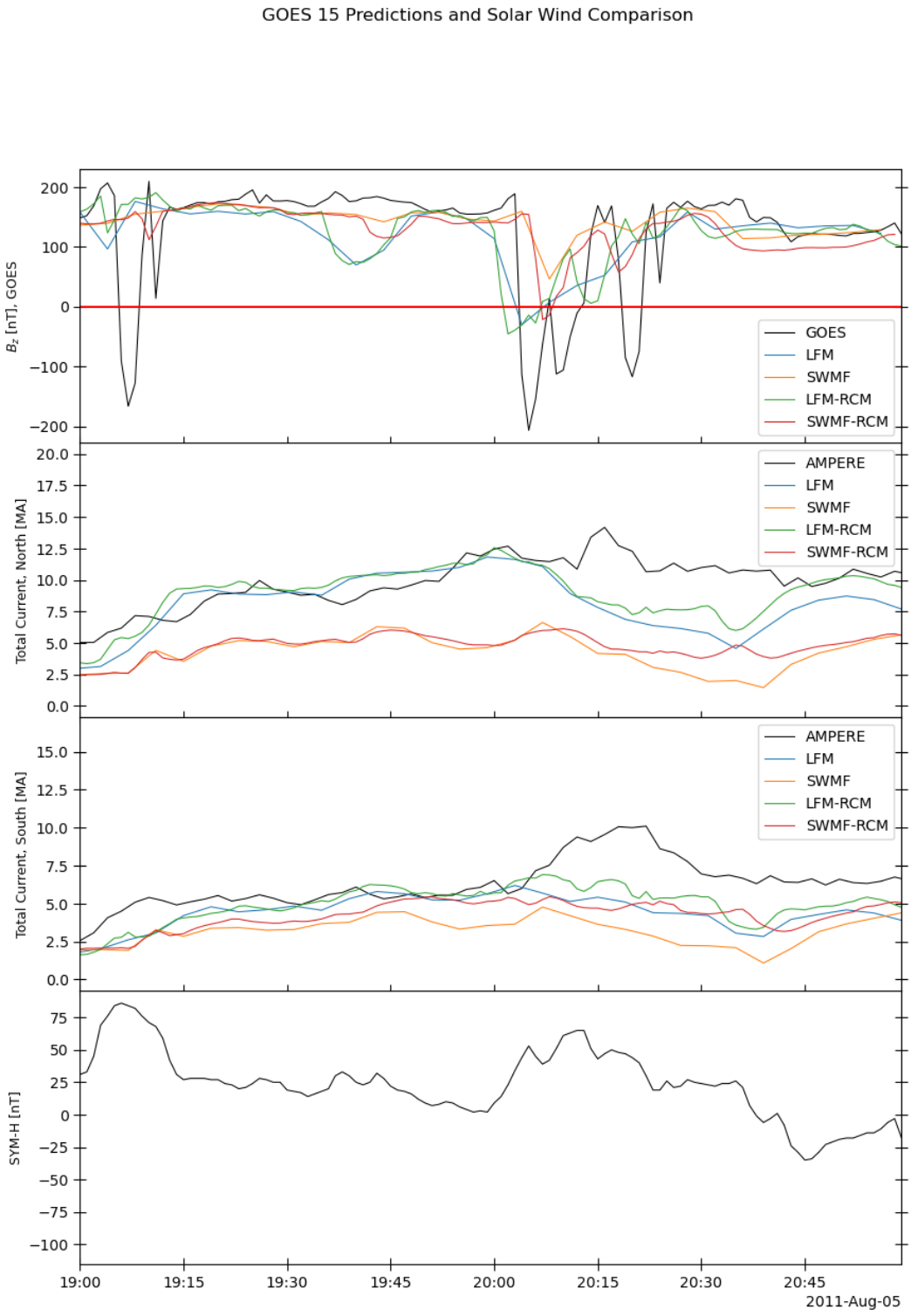

Figure 12. Same as Figure 11, but for 2011 August 5. The ring current had not yet become strong during the time of the magnetopause crossings.

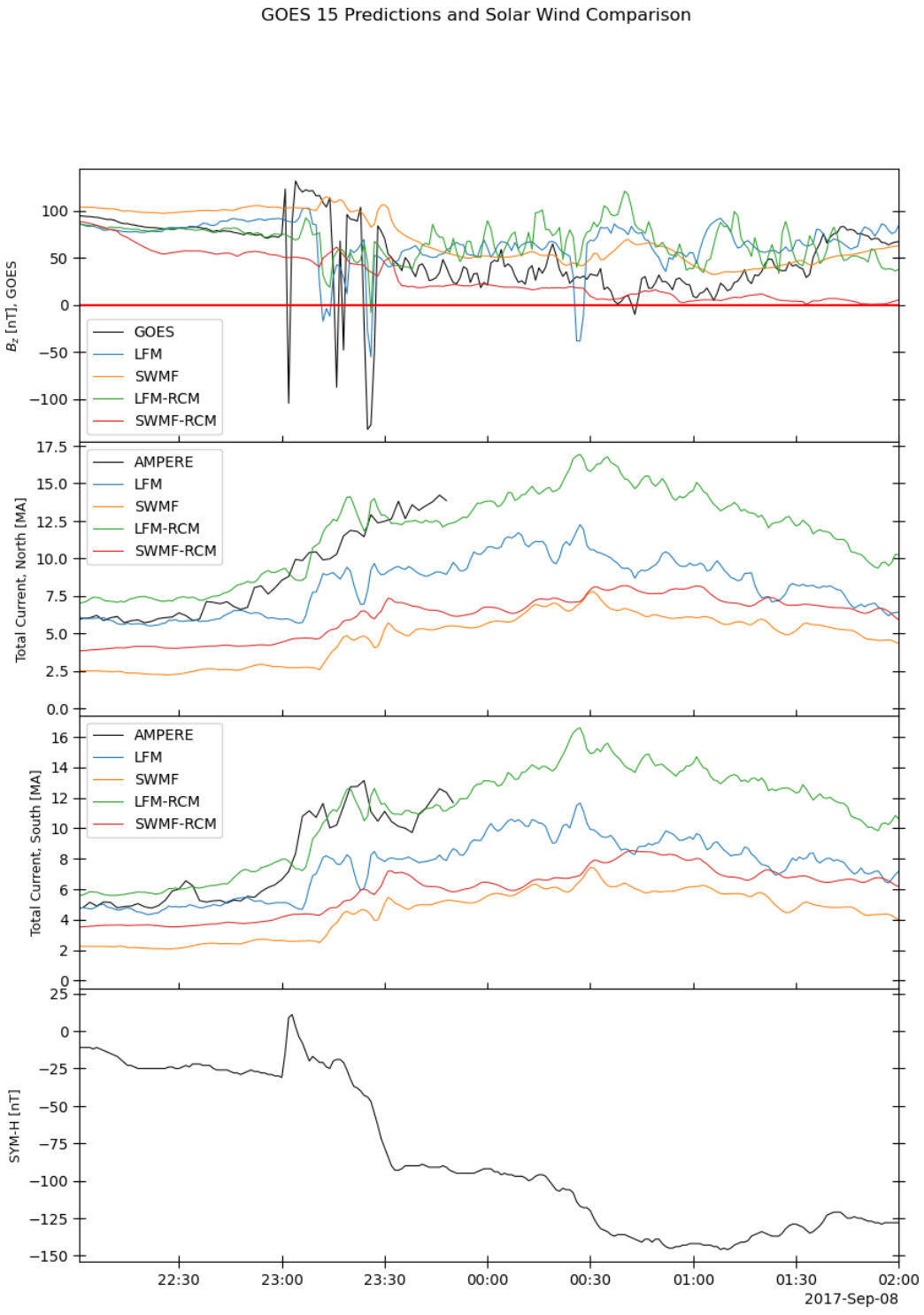

Figure 13. Same as Figure 11, but for 2017 September 7-8. AMPERE data are not available for 2017 September 8. The ring current had not yet become strong during the time of the magnetopause crossings.

LFM, right before 00:30 and further into the storm than the real crossings, is removed, but SWMF still misses the crossings altogether (Figure 13). The Birkeland current predictions for LFM are much improved, while those in SWMF still fall short of the AMPERE values.

The results of the LFM-RCM and SWMF-RCM runs for the 2015 June 22 storm do not display the expected effect of the ring current. With some small improvements, the predictions at the GOES locations are largely similar to those from the runs without the ring current. The Birkeland current magnitudes are somewhat improved, but the models still miss the peak in the southern hemisphere current around 20:00 UT. Additionally, adding RCM does not remove the increase in the currents of both hemispheres predicted shortly after 21:00 UT and corresponding with spurious GOES crossings in LFM, although it does, barely, remove the crossing in GOES 13, as shown in Figure 14.

4 Discussion

The inhomogeneous nature of the solar wind means that plasma features and IMF observed near L1 do not necessarily reach the magnetosphere. This is a well-known issue (Merkin et al., 2013), yet space weather forecasts must for the time being rely on point observations at L1 to characterize the solar wind. Since discrepancies large enough to significantly change predictions of magnetopause position exist in three out of four of the events here considered, it would be useful to have a quantitative idea of the probability that the solar wind in the OMNI dataset does not represent the solar wind that impacts the bow shock. A possible approach to such a study would compare OMNI data to observations from spacecraft like THEMIS B/C or Geotail, during periods when they are near the Earth-Sun line, to calculate the correlation of the two datasets.

Inaccuracies in the prediction of the field-aligned currents reduce the models' reliability when the magnetopause moves because of erosion of Earth's magnetic field. The investigations of the response of the MHD codes to southward turnings in the IMF have here been restricted to the consideration of the effect of the ring current on the Birkeland current predictions, but the nature of the modeled ionosphere must play a role as well. Further studies should consider the results of coupling more sophisticated ionosphere models to LFM and OpenGGCM or even of setting a range of constant Pedersen conductances for repeated simulation runs.

Including ring current physics tends to improve storm-time predictions of magnetopause location, especially when the movements of the magnetopause is caused by erosion of Earth's magnetic field due to a strong southward IMF component, but coupling RCM to the MHD codes does not completely solve the problem. On the one hand, a significant IMF B_y component can cause interhemispheric asymmetries in the ionosphere which may not necessarily be reproduced in the models, since MHD models coupled to RCM only couple the northern hemisphere to the ring current (Pembroke et al., 2012; Zeeuw et al., 2004). Introducing B_y changes the location of the ring current, moving it away from the equatorial plane either north or south, depending on the sign of B_y. If the models are not capturing all the B_y effects, the simulated ring current may not be in the correct location. Such an error could particularly affect predictions in the +Y sector, where the asymmetric inflation of the ring current can influence the location of the magnetopause.

During the storm of 2015 June 22, after 20:00 UT, the IMF had a very strong B_y component for several hours, during which time LFM predicted false magnetopause crossings by both GOES 13 and 15 (Figure 15). Adding the ring current to the LFM predictions removes the actual crossing at GOES 13, but the simulated satellite still approaches the boundary too closely. At this time, GOES 13 was well into the afternoon sector, so the ring current should have had a greater influence on magnetopause location in the re-

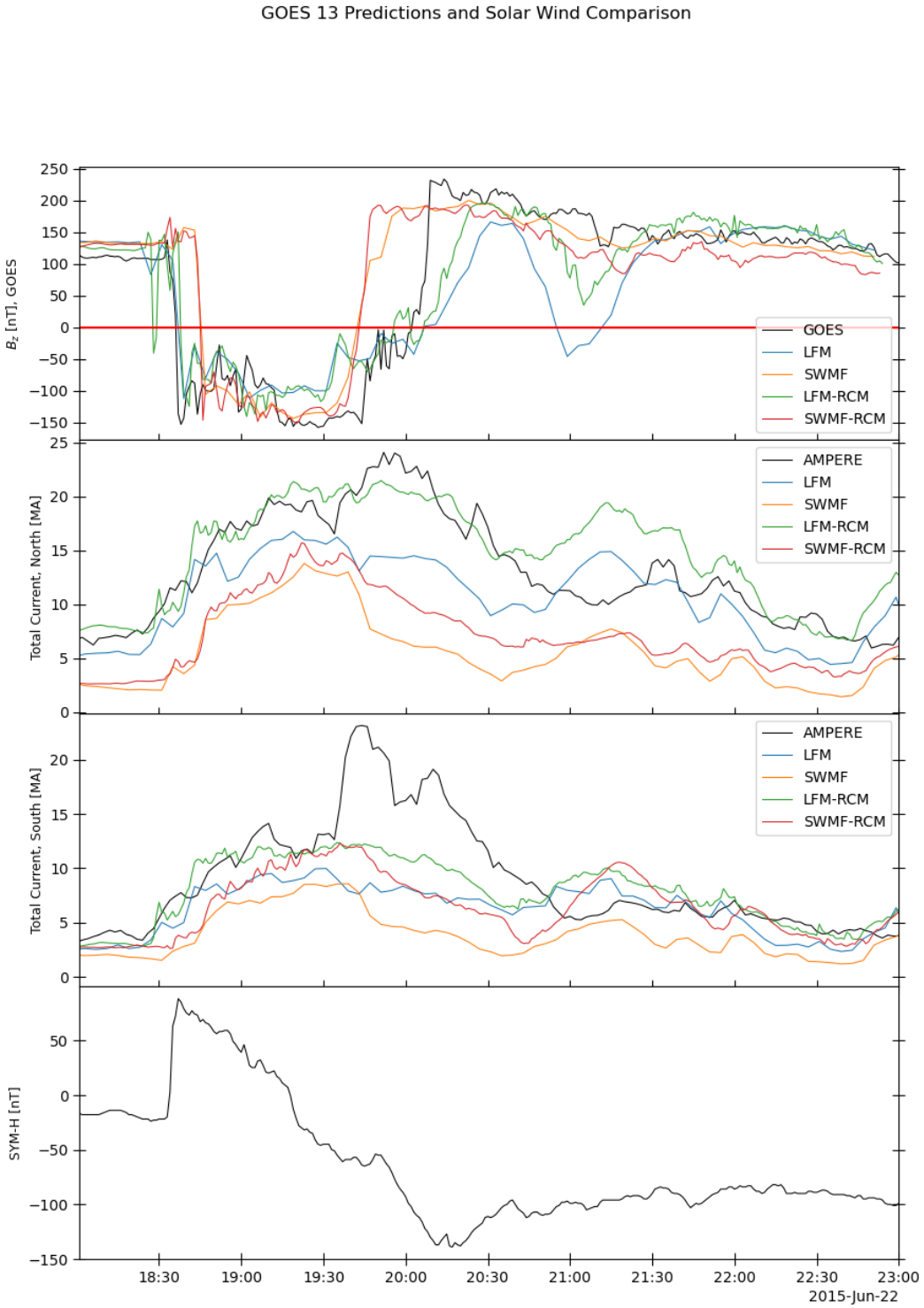

Figure 14. Same as Figure 11, but for GOES 13 on 2015 June 22. Although during the beginning of the real crossing the ring current is weak, it is strong by 19:30 UT.

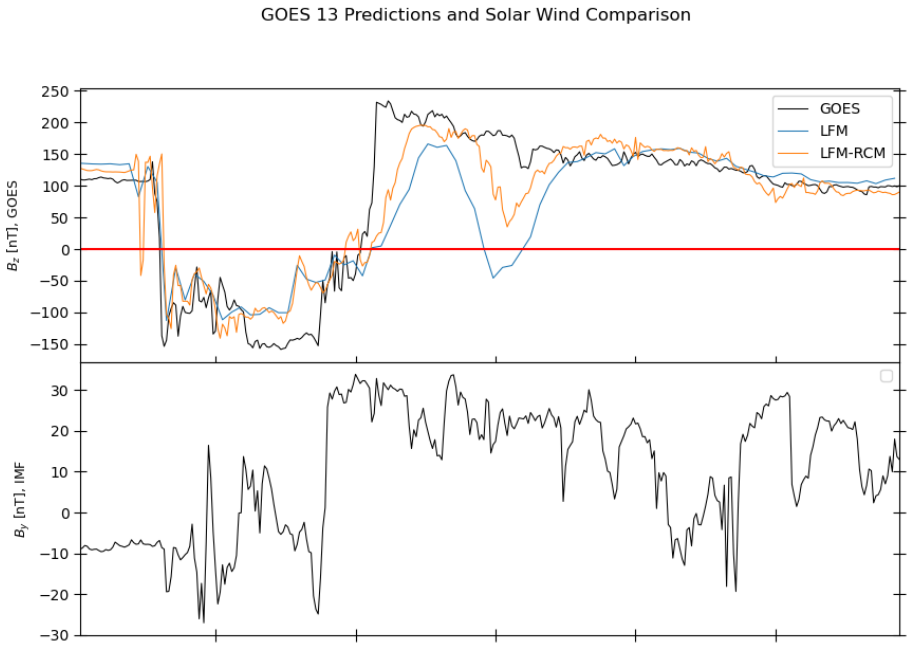

Figure 15. GOES 13 observations and the corresponding predictions by LFM and LFM-RCM, on 2015 June 22, with OMNI IMF B_y. During the time of the spurious crossing predicted by LFM, the IMF had a very strong, positive B_y component.

gion through which the spacecraft was passing. It seems possible that the enormous IMF B_y at the time was causing effects in the real magnetosphere that were not reproduced in the simulation, perhaps resulting in a modeled ring current that was in the wrong place.

5 Conclusions

In this study, four events during which the magnetopause moved in past geosynchronous orbit were selected and modeled with four different MHD codes. GOES 13 and 15 data were compared with simulation results at the GOES positions to analyze the ability of the models to predict magnetopause motion. There are two main causes of mistakes in the predictions. Firstly, the exact solar wind observed near the first Lagrange point does not always reach the magnetosphere, so using it as input for magnetosphere simulations can lead to false predictions of magnetopause motion. Secondly, although the models accurately predict the response of the magnetopause to changes in solar wind density, they sometimes struggle to calculate the Birkeland currents; this can lead to incorrect predictions of the erosion of Earth's magnetic field and the consequent motion of the magnetopause. The chances of correctly predicting magnetopause location during a storm are significantly improved by using a ring current model.

6 Open Research

GOES data were provided by NOAA (`https://satdat.ngdc.noaa.gov/`). OMNI and THEMIS data were provided by CDAWeb (NASA CDAWeb Development Team, 2019). Orbit plots were provided by SSCWeb (`https://sscweb.gsfc.nasa.gov/cgi-bin/Locator_graphics.cgi`). We thank the AMPERE team and the AMPERE Science Center for providing the Iridium derived data products (`http://ampere.jhuapl.edu/`).

Acknowledgments

We acknowledge the support of the US National Science Foundation (NSF) under grant 1916604. We also acknowledge the support of the National Aeronautics and Space Administration (NASA) under grants 80NSSC19K1670 and 80NSSC20K0606 (The Center for the Unified Study of Interhemispheric Asymmetries (CUSIA)).

Simulation results have been provided by the Community Coordinated Modeling Center at Goddard Space Flight Center through their public Runs on Request system (`http://ccmc.gsfc.nasa.gov`). The LFM Model was developed by John Lyon et al. at Dartmouth College/NCAR-HAO/JHU-APL/CISM. OpenGGCM was developed by Joachim Raeder and Timothy Fuller-Rowell at the Space Science Center, University of New Hampshire. GUMICS was developed by Pekka Janhunnen et al. at the Finnish Meteorological Institute. This work was carried out using the SWMF and BATS-R-US tools developed at the University of Michigan's Center for Space Environment Modeling (CSEM). The modeling tools described in this publication are available online through the University of Michigan for download and are available for use at the Community Coordinated Modeling Center (CCMC).

References

Bonde, R. E. F., Lopez, R. E., & Wang, J. Y. (2018). The effect of imf fluctuations on the subsolar magnetopause position: A study using a global mhd model. *Journal of Geophysical Research: Space Physics*, *123*(4), 2598-2604. doi: 10.1002/2018JA025203

Cramer, W., Raeder, J., Toffoletto, F., Gilson, M., & Hu, B. (2017, 04). Plasma sheet injections into the inner magnetosphere: Two-way coupled openggcm-rcm model results: Openggcm-rcm plasma sheet injections. *Journal of Geo-*

physical Research: Space Physics, *122*. doi: 10.1002/2017JA024104

Dmitriev, A., Suvorova, A., & Chao, J. (2011, 05). A predictive model of geosynchronous magnetopause crossings. *Journal of Geophysical Research: Space Physics*, *116*. doi: 10.1029/2010JA016208

Janhunen, P., Palmroth, M., Laitinen, T., Honkonen, I., Juusola, L., Facsko, G., & Pulkkinen, T. (2012). The gumics-4 global mhd magnetosphere-ionosphere coupling simulation. *Journal of Atmospheric and Solar - Terrestrial Physics*, *80*, 48–59. doi: 10.1016/j.jastp.2012.03.006

Lopez, R. E., Hernandez, S., Wiltberger, M., Huang, C. L., Kepko, E. L., Spence, H., ... Lyon, J. G. (2007, January). Predicting magnetopause crossings at geosynchronous orbit during the Halloween storms. *Space Weather*, *5*(1), 01005. doi: 10.1029/2006SW000222

Lyon, J., Fedder, J., & Mobarry, C. (2004, 10). The lyon-fedder-mobarry (lfm) global mhd magnetosphere simulation code. *Journal of Atmospheric and Solar-Terrestrial Physics*, *66*, 1333-1350. doi: 10.1016/j.jastp.2004.03.020

Maltsev, Y. P., Arykov, A. A., Belova, E. G., Gvozdevsky, B. B., & Safargaleev, V. V. (1996). Magnetic flux redistribution in the storm time magnetosphere. *Journal of Geophysical Research: Space Physics*, *101*(A4), 7697-7704. Retrieved from `https://agupubs.onlinelibrary.wiley.com/doi/abs/10.1029/95JA03709` doi: https://doi.org/10.1029/95JA03709

Maltsev, Y. P., & Lyatsky, W. B. (1975). Field-aligned currents and erosion of the dayside magnetosphere. *Planetary and Space Science*, *23*, 1257-1260.

Martyn, D. F. (1951, January). The theory of magnetic storms and auroras. *Nature*, *167*, 92-94.

Merkin, V. G., Anderson, B. J., Lyon, J. G., Korth, H., Wiltberger, M., & Motoba, T. (2013, August). Global evolution of Birkeland currents on 10 min timescales: MHD simulations and observations. *Journal of Geophysical Research (Space Physics)*, *118*(8), 4977-4997. doi: 10.1002/jgra.50466

Merkin, V. G., & Lyon, J. G. (2010). Effects of the low-latitude ionospheric boundary condition on the global magnetosphere. *Journal of Geophysical Research: Space Physics*, *115*(A10). doi: https://doi.org/10.1029/2010JA015461

NASA CDAWeb Development Team. (2019, April). *CDAWeb: Coordinated Data Analysis Web.* Astrophysics Source Code Library, record ascl:1904.006.

Pembroke, A., Toffoletto, F., Sazykin, S., Wiltberger, M., Lyon, J., Merkin, V., & Schmitt, P. (2012). Initial results from a dynamic coupled magnetosphere-ionosphere-ring current model. *Journal of Geophysical Research: Space Physics*, *117*(A2). Retrieved from `https://agupubs.onlinelibrary.wiley.com/doi/abs/10.1029/2011JA016979` doi: https://doi.org/10.1029/2011JA016979

Powell, K. G., Roe, P. L., Linde, T. J., Gombosi, T. I., & De Zeeuw, D. L. (1999). A solution-adaptive upwind scheme for ideal magnetohydrodynamics. *Journal of Computational Physics*, *154*(2), 284-309. Retrieved from `https://www.sciencedirect.com/science/article/pii/S002199919996299X` doi: https://doi.org/10.1006/jcph.1999.6299

Raeder, J., Larson, D., Li, W., Kepko, E. L., & Fuller-Rowell, T. (2008). Openggcm simulations for the themis mission. *Space Science Reviews*, *141*(1), 535–555.

Raeder, J., McPherron, R., Frank, L., Kokubun, S., Lu, G., Mukai, T., ... Slavin, J. (2001). Global simulation of the geospace environment modeling substorm challenge event. *Journal of Geophysical Research: Space Physics*, *106*(A1), 381–395.

Sibeck, D. G. (1995). Demarcating the magnetopause boundary. *Reviews of Geophysics*, *33*(S1), 651–655.

Sibeck, D. G., Lopez, R. E., & Roelof, E. C. (1991, April). Solar wind control of the magnetopause shape, location, and motion. *Journal of Geophysical Research*, *96*(A4), 5489-5495. doi: 10.1029/90JA02464

Toffoletto, F., Sazykin, S., Spiro, R., & Wolf, R. (2003, April). Inner magnetospheric modeling with the rice convection model. *Space Science Reviews*, *107*, 175-196. doi: 10.1023/A:1025532008047

Tóth, G., van der Holst, B., Sokolov, I. V., De Zeeuw, D. L., Gombosi, T. I., Fang, F., ... Opher, M. (2012, February). Adaptive numerical algorithms in space weather modeling. *Journal of Computational Physics*, *231*(3), 870-903. doi: 10.1016/j.jcp.2011.02.006

Tóth, G., Sokolov, I. V., Gombosi, T. I., Chesney, D. R., Clauer, C. R., De Zeeuw, D. L., ... Kóta, J. (2005). Space weather modeling framework: A new tool for the space science community. *Journal of Geophysical Research: Space Physics*, *110*(A12). Retrieved from `https://agupubs.onlinelibrary.wiley.com/doi/abs/10.1029/2005JA011126` doi: https://doi.org/10.1029/2005JA011126

Wiltberger, M., Lopez, R., & Lyon, J. (2003). Magnetopause erosion: A global view from mhd simulation. *Journal of Geophysical Research: Space Physics*, *108*(A6).

Wolf, R. A., Harel, M., Spiro, R. W., Voigt, G.-H., Reiff, P. H., & Chen, C.-K. (1982). Computer simulation of inner magnetospheric dynamics for the magnetic storm of july 29, 1977. *Journal of Geophysical Research: Space Physics*, *87*(A8), 5949-5962. Retrieved from `https://agupubs.onlinelibrary.wiley.com/doi/abs/10.1029/JA087iA08p05949` doi: https://doi.org/10.1029/JA087iA08p05949

Zeeuw, D., Sazykin, S., Wolf, R., Gombosi, T., Ridley, A., & Toth, G. (2004, 12). Coupling of a global mhd code and an inner magnetosphere model: Initial results. *Journal of Geophysical Research: Space Physics*, *109*. doi: 10.1029/2003JA010366